

## Measuring the Characteristics of Short-Period Internal Waves Using an Array of Drifting Thermoprofiling Buoys

E. I. Svergun<sup>1, ✉</sup>, A. V. Zimin<sup>1, 2</sup>, **S. V. Motyzhev<sup>3, 4</sup>**,  
E. G. Lunev<sup>3, 4</sup>, A. P. Tolstosheev<sup>3, 4</sup>, M. S. Volikov<sup>3, 4</sup>

<sup>1</sup> Shirshov Institute of Oceanology, Russian Academy of Sciences, Moscow, Russian Federation

<sup>2</sup> Saint Petersburg State University, Saint Petersburg, Russian Federation

<sup>3</sup> Sevastopol State University, Sevastopol, Russian Federation

<sup>4</sup> Marlin-Yug LLC, Sevastopol, Russian Federation

✉ Egor-svergun@yandex.ru

### Abstract

**Purpose.** Technical characteristics of a mobile rapidly deployable autonomous hydrophysical measuring system based on an array of drifting buoys, as well as the method for analyzing the obtained measurement data are described to study the characteristics of short-period internal waves.

**Methods and Results.** The developed system is based on the autonomous free-drifting surface thermoprofiling buoys and the automatic receiving station. Each of the buoys is equipped with a measuring line with eighteen temperature sensors and a hydrostatic pressure sensor, a global positioning receiver, a data collection system and a satellite modem for data transmission. The receiving station consists of the information receiving unit, satellite communication antennas and global positioning system, as well as a personal computer with specialized software. A method for assessing the characteristics of short-period internal waves based on the observational data from autonomous hydrophysical system is presented. The novelty of the method consists in determining the time difference between the arrivals of internal wave trains at different measuring lines based on the local maxima of moving dispersion at the pycnocline depth. The examples of analyzing the observational data obtained in the large thermostratified lake (Lake Onega) and in the sea (Kara Gate Strait) are presented. The obtained and submitted estimates of phase velocity and direction of the propagation of internal waves are compared to the simplest model estimates.

**Conclusions.** The developed software and hardware packages significantly simplify the process of studying the characteristics of short-period internal waves in relatively large lakes and distant areas of the World Ocean. The examples of system application have shown its versatility. In future, the buoy group can be supplemented with new buoys with additional sensors that will expand the possibilities for analyzing observational data.

**Keywords:** water temperature, measurement methods, *in situ* measurements, distributed measuring systems, short-period internal waves, signal processing, Lake Onega, Kara Sea

**Acknowledgements:** Measurements in the Kara Sea were carried out within the framework of scientific and educational program “Floating University” (agreement No. 075-01593-23-06). Measurement results were processed within the framework of state assignment of IO, RAS No. FMWE-2024-0028.

**For citation:** Svergun, E.I., Zimin, A.V., Motyzhev, S.V., Lunev, E.G., Tolstosheev, A.P. and Volikov, M.S., 2025. Measuring the Characteristics of Short-Period Internal Waves Using an Array of Drifting Thermoprofiling Buoys. *Physical Oceanography*, 32(3), pp. 392-407.

© 2025, E. I. Svergun, A. V. Zimin, S. V. Motyzhev, E. G. Lunev, A. P. Tolstosheev, M. S. Volikov

© 2025, Physical Oceanography



## Introduction

One of the important current problems in ocean physics is the need to monitor the short-term and submesoscale variability of ocean hydrological field characteristics to determine the geographical features of their contribution to dissipative processes in various areas of the continental shelf [1]. The main difficulty in solving this problem lies in obtaining high-resolution measurements in both space and time simultaneously [2]. A similar problem in local water areas can be solved, for example, using clusters of temperature meters distributed across the area, such as moored chains (thermochains) [3] or integrated sensors [4]. However, setting up and removing moored stations is associated with significant difficulties and risks. Groups of thermochains (thermolines) lowered from [5] or towed behind a vessel [6] can also be used.

Such approaches can be applied anywhere in the World Ocean. However, given the significant labor intensity and cost of such work, questions naturally arise about economic efficiency, selection of areas and the timing of observations. The answers to these questions led to the idea of using autonomous surface-drifting SVP-type buoys. Their successful use in programs such as GDP (Global Drifting Program)<sup>1</sup> and UpTempO<sup>2</sup> confirmed their high efficiency in studying the active layer of the ocean [7]. Therefore, temperature-profiling drifting buoys (SVP BTC60/GPS/ice), which were used to study the Arctic region in the UpTempO program and for which manufacturing experience is available to domestic manufacturers [8], can be considered a prototype for an inexpensive, mobile monitoring system.

The improvement of this type of buoy and the unification of several buoys into a single measuring cluster [9, 10] enabled the development of a prototype monitoring system for short-period variability in the temperature of the active layer of the World Ocean. This prototype enables the characteristics of the field of short-period internal waves (SIW) to be monitored at any point in the World Ocean and the data obtained to be transmitted and processed promptly. The buoy observation facilities are adapted for year-round use in the Arctic. The integrated information system ensures the collection of measurement data, their transmission through the buoy-user communication channels, and the processing and presentation of data at a timescale close to real time. This makes it possible to determine the amplitudes, periods, speeds and directions of propagation of SIW, based on the time difference between wave packets arriving at various buoys in the array.

In [11] it is noted that similar systems were used in 1980–1990s, but their technical imperfections resulted in the method being abandoned. The new generation of systems is now being used more widely to record the spatial characteristics of internal waves in expeditionary practice. Therefore, the methodological basis for their use is only beginning to form. Specialized software needs to be developed from scratch to process data obtained from a specific buoy system.

---

<sup>1</sup> ARGOS. *Global Drifter Program*. [online] Available at: <https://www.argos-system.org/project/global-drifter-program/> [Accessed: 05 September 2024].

<sup>2</sup> UpTempO. *Measuring the Upper Layer Temperature of the Polar Oceans*. [online] Available at: <http://psc.apl.washington.edu/UpTempO/> [Accessed: 05 September 2024].

This paper aims to provide the technical characteristics of a rapidly deployable, autonomous, hydrophysical measuring system based on an array of drifting buoys. It also describes the method used to analyze the obtained measurement data in order to study the characteristics of short-period internal waves.

### Materials and methods

**Array of the drifting buoys used.** To record the SIW characteristics, the Volna-DS-01 hydrophysical measuring system (drifting system) manufactured by Marlin-Yug (Russia) was used. It consists of at least three autonomous, freely drifting Volna-DB-01 surface temperature-profiling buoys (drifting buoys) (the number can be increased several times), and the station for automatic data reception from Volna PS-01 drifting buoys (receiving station). Fig. 1, a shows a diagram of the Volna-DS-01 hydrophysical measuring system.

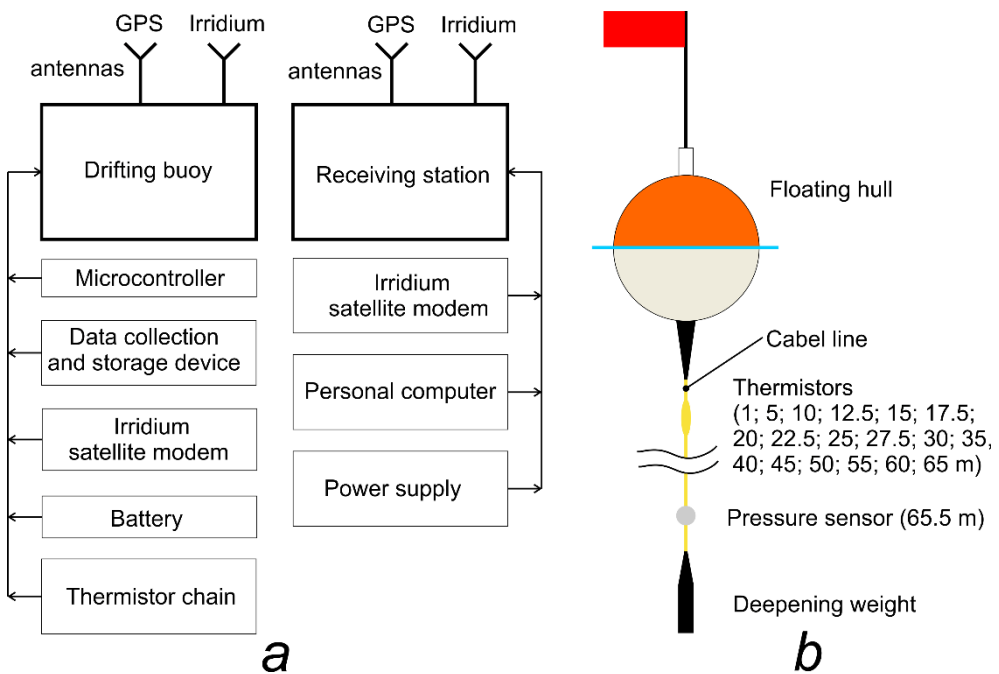


**Fig. 1.** Volna-DS-01 hydrophysical measuring system: *a* – diagram of the components (Volna-DB-01 drifting buoy and Volna-PS-01 receiving station); *b* – schematic diagram of a drifting buoy

Each drifting buoy (Fig. 1, *b*) consists of a floating hull and a measuring line. The hull is made of two polycarbonate hemispheres, hermetically connected by a flange mount. The upper part of the hull contains a hermetically sealed compartment with a USB A interface for connecting a flash drive. A flagpole with a red signal flag is installed on the hull and is equipped with a line to facilitate setting up and retrieving the drifting buoy.

The hermetically sealed hull contains power supply elements that provide at least 1,200 hours of continuous operation, as well as a real-time system controller, a GNSS GLONASS/GPS module with an antenna and an Iridium satellite modem with an antenna. The GNSS module determines the coordinates of each drifting buoy

and synchronizes the measurement time. The satellite modem provides prompt transmission of the geographic coordinates of each drifting buoy with a resolution of 10 minutes. Temperature and hydrostatic pressure profile measurements, buoy power source parameters and additional diagnostic information are transmitted synchronously with the geographic coordinates. The floating hull is equipped with a magnetic power switch and light indicators for the operating mode of the measuring system and the status of satellite data transmission.

The measuring line consists of a twisted pair of cables and a supporting rope. The cable contains 18 digital temperature sensors and a hydrostatic pressure sensor. The readings from these sensors are used to determine their actual horizons when the measuring line deviates from the vertical. The nominal horizons of the sensors are shown in Fig. 1. The design of the temperature sensor housings ensures they are easily washed by the surrounding water, reducing the time constant. A deepening weight is located at the lower end of the measuring line.

The Volna-PS-01 receiving station comprises a data reception unit, Iridium and GNSS satellite system antennas, and a laptop with specialized software. The data reception unit contains an Iridium satellite system modem and a controller, as well as an atmospheric pressure meter designed to correct the readings of the hydrostatic pressure sensors on the buoys. The GNSS antenna includes a BU-353s4/BR-355s4 (GlobalSat) GPS receiver. The software displays the information received by the station in graphic (temperature distribution by depth and drift map) and text (buoy coordinates and station coordinates and speed) formats. The receiving station and the drifting buoys can be in any relative position, which enables the system status to be monitored both from the vessel and from the shore station.

The table below provides information about the characteristics of the sensors used in the drifting system. The minimum possible measurement interval is 10 sec.

#### Technical and metrological characteristics of the drifting system sensors

Measured parameter	Measurement range	Measurement error	Resolution	Time constant
Temperature	-2...35 °C	±0.05 °C	0.015 °C	15 sec
Hydrostatic pressure	850...10000 GPa	±0.4 % of the measured value	1 GPa	2 sec
Location coordinates	Latitude: -90°...+90°, Longitude: 0°...360°	Hit radius of 95 % of locations does not exceed 10 m	0.00001°	–

**Examples of system application.** Fig. 2 shows the location where the Volna-DS-01 hydrophysical measuring system was used.

Tests of the system were carried out in Kondopozhskaya Bay and Bolshoe Onego Bay in Lake Onega in June 2022, as part of the Karelian Scientific Center's expedition aboard the R/V *Ecolog* (point 1 in Fig. 2). Lake Onega was chosen as a test site to minimize the risks of equipment failure or loss and to enable the use of a drifting system to record SIW characteristics in a large stratified water body.

Marine measurements using a drifting system were carried out in July 2023 and 2024 in the Kara Sea as part of the Floating University expeditions on

the R/Vs *Dalniye Zelentsy* and *Professor Molchanov*. The drifting system was deployed in the Kara Gate Strait (points 2 and 3 in Fig. 2), above the Novozemelsky Trench (point 4 in Fig. 2) and near Zhelaniya Cape (point 5 in Fig. 2).

A total of six measurements were taken in Lake Onega with a total duration of 46 hours. The duration of each measurement ranged from 3 to 10 hours. An example of a buoy drift map is shown in the inset of Fig. 2. Five measurements were taken in the Kara Sea, each lasting between 6 and 12 hours, for a total duration of 37 hours.

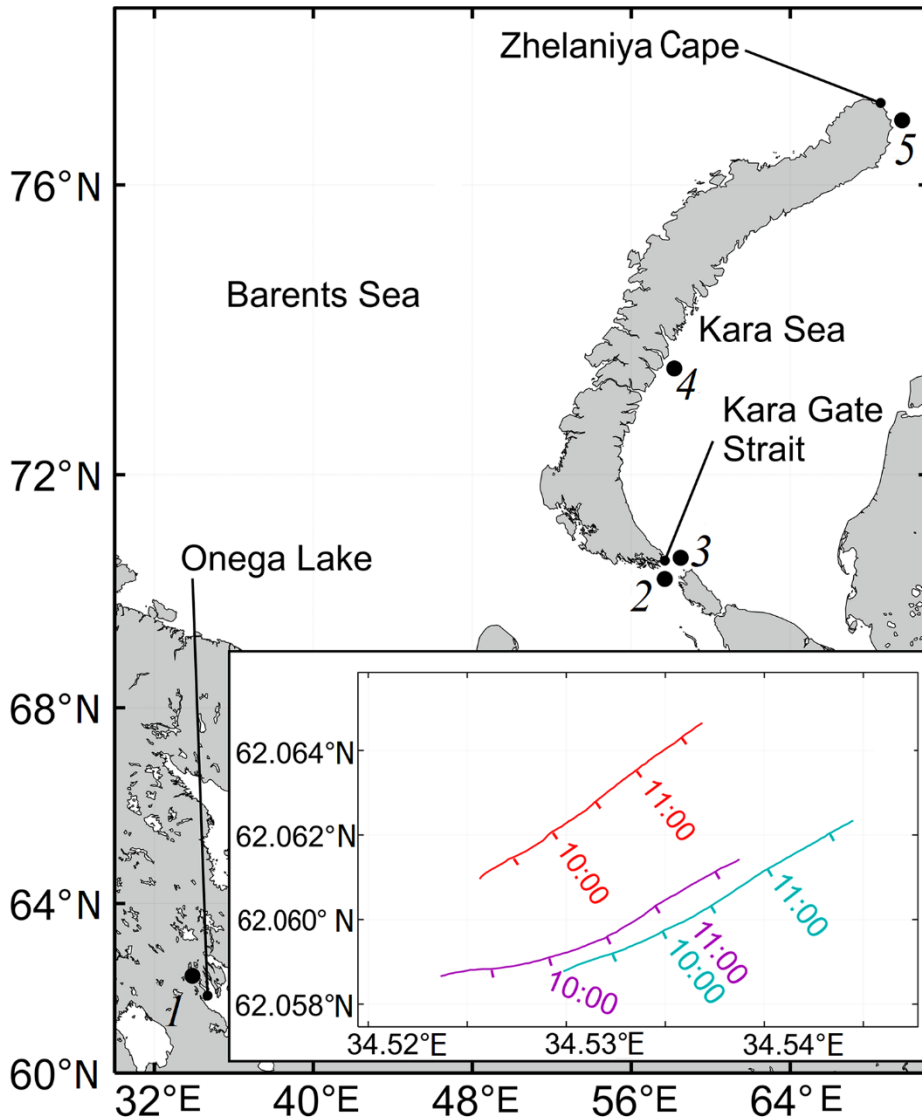


**Fig. 2.** Map of application of the hydrophysical measuring system (1 – Lake Onega; 2, 3 – Kara Gate Strait; 4 – Novozemelsky Trench; 5 – Zhelaniya Cape); *inset* – map of the buoys B<sub>1</sub>–B<sub>3</sub> drifts (1–3 are the manufacturer serial numbers) in Lake Onega on June 16, 2022 (red line shows buoy B<sub>1</sub>, purple line – buoy B<sub>2</sub> and turquoise one – buoy B<sub>3</sub>)

Drifting buoys were installed and removed manually from a working boat at sea states of up to three to avoid damaging the floating housing. During the measurements, each drifting buoy collected data on the vertical temperature distribution in a 1–65 m layer and its own drift coordinates. These were supplemented by the results of control (background) measurements taken by CastAway (USA), CTD48M (Germany) and SBE19plus V2 (USA) CTD probes from other vessels.

The paper will consider as an example the results of recording SIW characteristics in Lake Onega in June 2022 (Fig. 2, inset) and in the eastern part of the Kara Gate Strait in July 2023.

### **Methodology for estimating SIW characteristics using drifting system data.**

In order to record the speed and direction of SIW propagation, simultaneous measurements must be carried out at the location of at least three spaced-apart points. These SIW characteristics are usually assessed based on the time difference between wave packets arrivals at measuring devices positioned at the vertices of a triangle [6]. Therefore, the accuracy of propagation speed and direction estimates depends on the accuracy of determining the arrival delay time of a wave packet.

Various methods can be used to estimate delay time. In [5, 11, 12, 13], the delay time is estimated visually from the temperature fluctuation records directly. This method is effective when clearly distinguishable soliton-like waves are present in the records. However, in the presence of successive wave packets with a complex structure in the records, applying this method may be difficult. Another method of delay time estimation using the cross-correlation function maxima is described in [4, 6]. This method is applicable when the measuring devices are located at the vertices of a triangle, where the side length is much shorter than the length of the recorded waves. However, this configuration is not always convenient for implementation. The delay time can be determined using the integral temperature maxima [14] or the temperature change rate maxima at a certain horizon [3]. However, these methods are mainly described for use with large-amplitude and soliton-like waves.

This paper uses the moving dispersion estimate [15] of the isotherm depth to estimate the arrival delay time of wave packets. The moving dispersion method has previously been used to estimate fluctuations in various ionospheric parameters [16], geochemical parameters [17], and ocean current velocities [9, 18]. Since the moving dispersion reflects local changes in time series properties, its maxima correspond well to solitons and SIW packets.

Let us now take a closer look at the algorithm developed for processing the measurement data of the Volna-DS-01 drifting system (Fig. 3, *a*). The left-hand column of the block diagram shows the processing of data obtained from the vessel (background) and from buoys; the rest of the columns show the data only from the array of drifting buoys.

In the first stage of data analysis, when calculating the moving dispersion, it is necessary to determine the optimal window for the calculation of dispersion at each step. In the present paper, the optimal window was calculated as the ratio of the average buoy-to-buoy distance (based on their geographic coordinates) to the phase velocity of the internal waves, using the two-layer approximation [19] and

background CTD probing data (see the left-hand column of the block diagram in Fig. 3, *a*). The optimal window essentially represents the minimum time during which a wave will propagate from one drifting buoy to another. If the phase velocity is underestimated, the optimal window may exceed the period of the recorded waves. Therefore, the optimal window can also be estimated by calculating the minimum period of the internal waves in the temperature fluctuation record. However, it should be noted that the true period of the waves is distorted by buoy drift due to the Doppler effect.

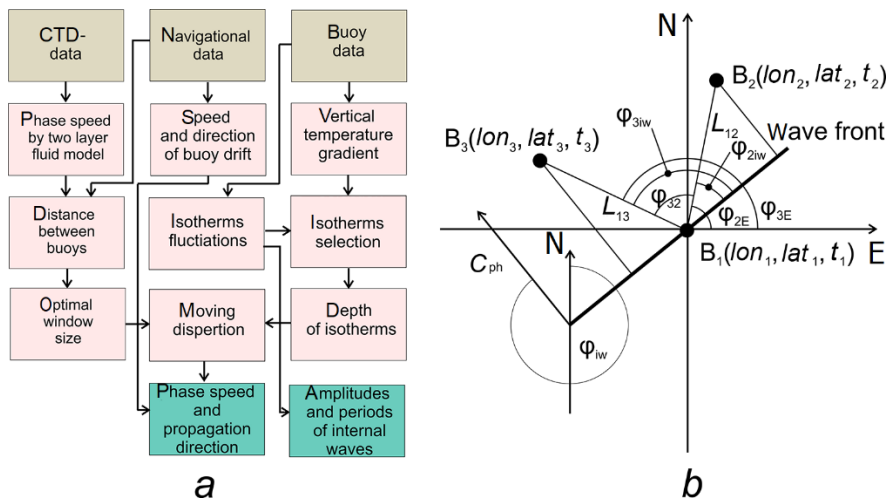


**Fig. 3.** Algorithm for calculating the SIW characteristics based on the drifting system measurements: *a* – block diagram of the algorithm (beige color shows initial data, pink – intermediate results, green – final results); *b* – graph for determining the SIW velocities and directions (letters *N* and *E* indicate the directions to the north and east, large dots labeled *lat* and *lon* show the buoy geographical locations at the time of wave packet recording, and signatures  $B_1$ ,  $B_2$  and  $B_3$  indicate the order of wave packet recording by the buoys of the drifting system where  $B_1$  is the buoy that first recorded the wave packet)

Fig. 3, *a* shows the algorithm for calculating SIW characteristics in the middle and right columns of the block diagram. It should be noted that the accuracy and efficiency of time difference estimation between the wave packet arrivals, based on moving dispersion maxima, is affected by the choice of an isotherm for analysis. The isotherm is selected in the layer with the maximum vertical temperature gradient, where the depth experiences the greatest amplitude fluctuations. Then, with a constant step size equal to the discreteness of the measurements, the depth values are calculated. SIW amplitudes and periods are then determined from these values in accordance with the methodology [20].

The moving dispersion of the isotherm depth is calculated by taking into account the optimal window estimates, and is normalized to the maximum value to facilitate subsequent joint analysis. The graphs showing the temporal variability of the moving dispersion illustrate visual registration of successive local maxima that occur close together in time for different buoys in the drifting system. Moreover, typically, the delay between local dispersion maxima for one pair of buoys out of three is greater than for the other pair.

Next, the positions of the local maxima are validated by direct comparison of the moving dispersion graphs with the isotherm fluctuation records. Firstly, based on the local maxima of the moving dispersion, the order of wave packet recording by the system buoys is determined. Secondly, the moments of wave packet recording by each buoy in the system are determined.

Then, taking into account the distance between the buoys (calculated using their geographic coordinates), the SIW phase velocity is determined [11]:

$$C_{\text{ph}} = \frac{L_{12} \sin \varphi_{2\text{iw}}}{t_2 - t_1} = \frac{L_{13} \sin \varphi_{3\text{iw}}}{t_3 - t_1}, \quad (1)$$

where  $L_{12}$  is the distance between  $B_1$  and  $B_2$  buoys;  $L_{13}$  is the distance between  $B_1$  and  $B_3$  buoys;  $t_1, t_2, t_3$  is the time of wave packet registration by  $B_1, B_2, B_3$  buoy sensors, respectively;  $\varphi_{2\text{iw}}$  is the angle between the wave front line passing through  $B_1$  point and the direction from  $B_1$  point to  $B_2$  point, determined by the following formula

$$\varphi_{2\text{iw}} = \arctg \left( \pm \frac{\sin \varphi_{32}}{\frac{(t_3 - t_1)L_{12} - \cos \varphi_{32}}{(t_2 - t_1)L_{13}}} \right), \varphi_{3\text{E}} > < \varphi_{2\text{E}},$$

where  $\varphi_{32}$  is the angle between the directions from  $B_1$  point to  $B_2$  and  $B_3$  point;  $\varphi_{2\text{E}}$  is the angle between the directions from  $B_1$  point eastward to  $B_2$  point;  $\varphi_{3\text{E}}$  is the angle between the directions from  $B_1$  point eastward to  $B_3$  point;  $\varphi_{3\text{iw}}$  is the angle between the wave front line passing through  $B_1$  point and the direction from  $B_1$  point to  $B_3$  point, determined by the following formula

$$\varphi_{3\text{iw}} = \varphi_{2\text{iw}} \pm \varphi_{32}, \quad \varphi_{3\text{E}} >> \varphi_{2\text{E}}.$$

The SIW propagation direction (Fig. 3b) is determined by the formula [11]

$$\varphi_{\text{iw}} = 2\pi + \varphi_{2\text{iw}} - \varphi_{2\text{E}}. \quad (2)$$

There are also other expressions for calculating SIW characteristics [3, 6]. The expressions from [11] were chosen because the calculations using these expressions do not impose strict requirements on the relative position of the buoys, nor do they require a transition to another coordinate system.

Expressions (1) and (2) are used to calculate the speed and direction of wave propagation in a moving reference system associated with a drifting system. To obtain absolute estimates of these values, the vector sum of the wave speed and drift speed vectors is calculated. It is assumed that the buoys are drifting at the same speed when the wave packet is recorded.

The advantage of the method described in [11] is that the measuring system elements do not need to be rigidly fixed in space. The distance between the elements can be arbitrary and vary depending on the spatial scale of the phenomena being studied. The algorithm for processing the measurement results is implemented in the Matlab environment. The main data processing operations are accompanied by the graphic and text output.

## Results and their discussion

**SIW characteristics in Lake Onega based on drifting system measurements.** The measurement results of June 16, 2022 are given below as an example of the drifting system's use in Lake Onega. The system was deployed over depths of about 36 m in Bolshoe Onego Bay. To ensure stable operation of the drifting system, the working length of the thermal lines was reduced to 30 m by winding the lower part into coils. The distance between the system buoys was  $\sim 300$  m, and the drift velocity varied from 0.05 to 0.1 m/s. According to the background CTD probing data, stable temperature stratification was observed. The upper quasi-homogeneous layer had a thickness of 4 m, and the thermocline layer was located in the layer from 4 to 10 m, coinciding with the pycnocline position. The temperature gradient in the thermocline reached  $0.9\text{ }^{\circ}\text{C/m}$ , corresponding to a density gradient of  $0.08\text{ kg/m}^4$ .

Fig. 4 shows fragments of the measurement results in Lake Onega.

According to the data from each of the three buoys in the layer from 4 to 10 m, a clearly expressed wave packet with wave amplitudes of  $\sim 1$  m and periods of 10–15 min is noted in the records of isotherm fluctuations (Fig. 4, *a*). Based on these records, it is difficult to visually identify the arrival time of the packet at the drifting system buoys. Given the 276 m distance between the buoys and a phase velocity of 0.12 m/s according to the dispersion relation for a two-layer medium, the optimal window of the moving dispersion is 36 min. However, this exceeds the maximum period of the recorded fluctuations. Therefore, the optimal window of moving dispersion was set to the minimum wave period of 5 min.

The moving dispersion calculation for the  $10\text{ }^{\circ}\text{C}$  isotherm depth (thick black line in Fig. 4, *a*), selected based on the maximum vertical temperature gradient, demonstrates successive maxima (Fig. 4, *b*), which corresponds well to the leading waves in the packet when compared with the isotherm fluctuation records. The first local maximum of the moving dispersion ( $t_1$ ) was recorded at buoy 3 at 10:05 (UTC), the second ( $t_2$ ) – at buoy 2 at 10:06, and the third ( $t_3$ ) – at buoy 1 at 10:18.

Using the buoy position data, the phase velocity (0.33 m/s) and propagation direction ( $350^{\circ}$ ) of the leading wave of the packet were estimated in the reference system associated with the moving buoys using expressions (1) and (2), respectively. Taking into account the drift speed of the buoys of 0.08 m/s and the drift direction of  $38^{\circ}$ , the resulting wave packet propagation speed is 0.34 m/s in the direction of  $2^{\circ}$ .

The obtained direction of wave packet propagation is consistent with the spatial position of the local maxima of the normalized moving dispersion (Fig. 4, *c*), the order of wave packet registration, and the estimated time difference between wave packets arriving at the system buoys. The SIW propagation velocity obtained from processing the drifting system data is three times higher than the phase velocity estimated using two-layer stratification (0.34 m/s versus 0.12 m/s). This difference is probably due to the significant nonlinearity of the registered wave packet, or to the fact that the two-layer approximation is not entirely suitable for describing the velocity of internal waves in shallow, weakly stratified waters.

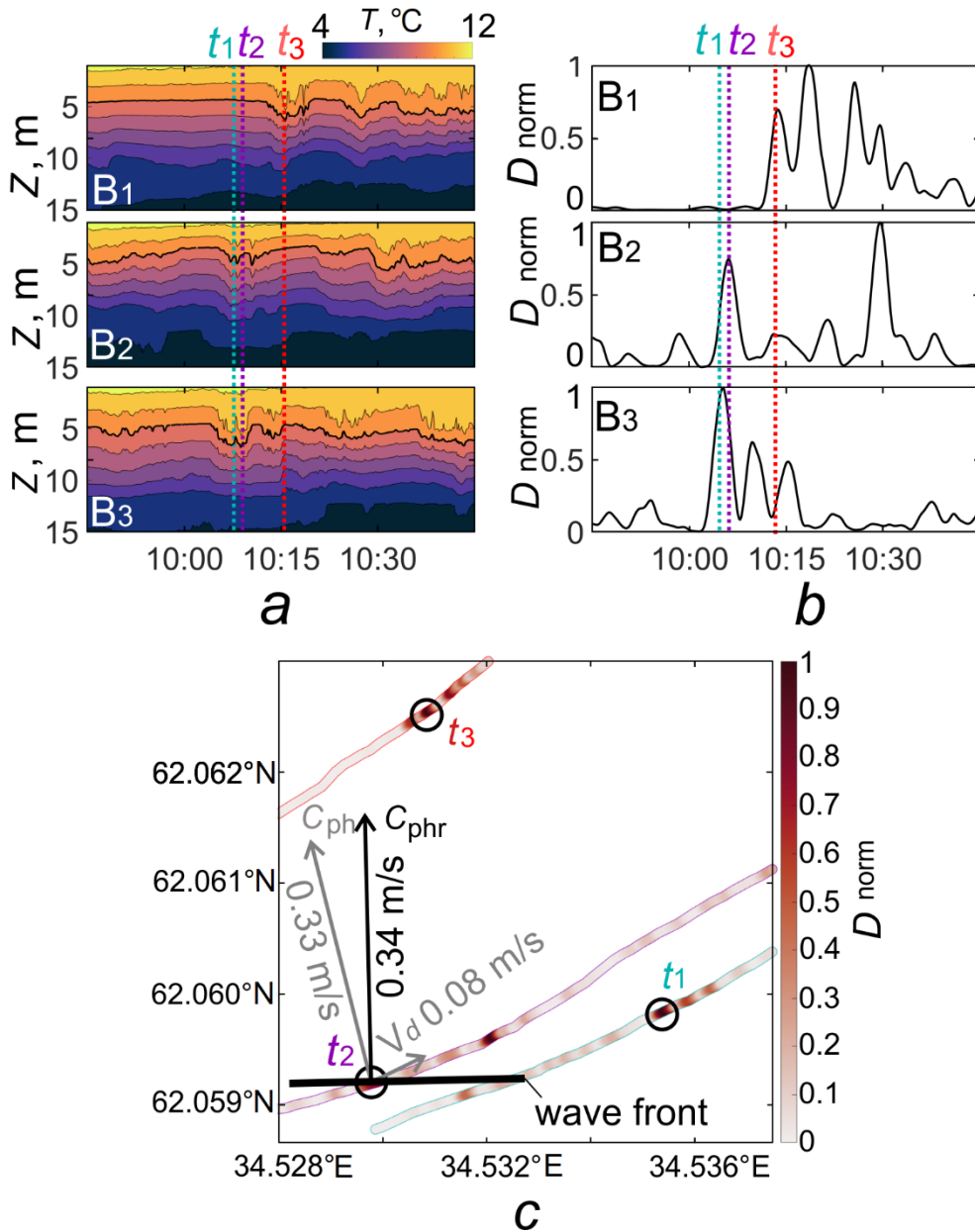


**Fig. 4.** Fragments of the measurement results obtained at R/V *Ecolog* in Lake Onega in June 2022: *a* – records of isotherm fluctuations for three buoys of the drifting system (red dashed line is buoy B1, purple dashed line – buoy B2, turquoise dashed line – buoy B3;  $t_1$ ,  $t_2$ ,  $t_3$  are the designations for the moments of the wave packet arriving at the buoys of the drifting system); *b* – time variations of the moving dispersion normalized to its maximum value for the 10 °C isotherm depths with a 5 min window; *c* – map of the moving dispersion distribution along the buoy drift trajectories with the vectors of buoy drift velocities and SIW phase speeds ( $C_{ph}$  is the phase speed of leading packet wave in the coordinate system related to the moving buoys,  $V_d$  is the buoy drift velocity and  $C_{phr}$  is the resulting phase speed)

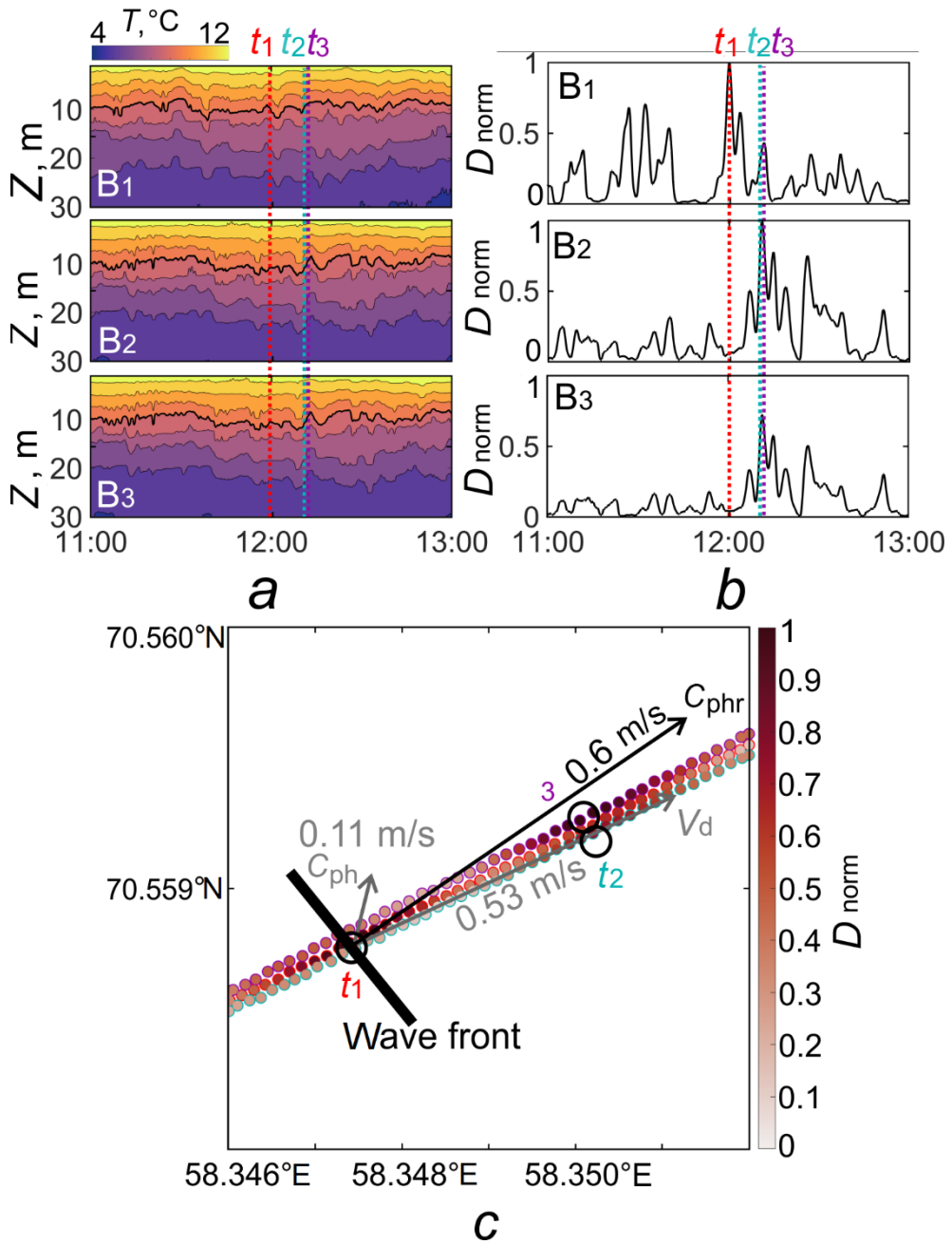


**Fig. 5.** Fragments of the measurement results obtained at R/V *Dalnie Zelentsy* in the Kara Gate Strait in July 2023 (see designations in Fig. 4): a – records of the isotherm fluctuations for three buoys of the drifting system; b – time variations of the moving dispersion normalized to its maximum value for the 9 °C isotherm depths with a 4 min window; c – map of the moving dispersion distribution along the buoy drift trajectories with the vectors of buoy drift velocities and SIW phase speeds (designations are as in Fig. 4)

It should be noted that the relationship between the velocities of linear and nonlinear waves is often discussed in the context of the Kortweg – de Vries (KdV) theory, describing the behavior of nonlinear waves, including solitons [21]. According to this theory, the velocity of nonlinear waves depends on their amplitude, whereas the velocity of linear waves is determined solely by the properties of the medium (stratification and depth).

**SIW characteristics in the Kara Sea according to drifting system measurements.** Let us consider the processing of drifting system measurements in the Kara Gate Strait on July 16, 2023 as an example. The system buoys were installed in the northeastern part of the strait (see Fig. 2), at depths of around 80 m and at a distance of about 140 m from each other. According to background sounding data, pronounced stratification close to a two-layer structure was revealed. The upper quasi-homogeneous layer, which was 5 m thick, and the lower layer were separated by a pycnocline in the 5–11 m layer, which had a density gradient of about  $0.42 \text{ kg/m}^4$ . The positions of the pycnocline and thermocline coincided. Given this stratification and in accordance with the dispersion relation for a two-layer medium, the phase velocity is 0.6 m/s.

Fig. 5 shows fragments of the measurement results in the Kara Gate Strait.

The records of isotherm fluctuations (Fig. 5, *a*) indicate the presence of SIW in a layer from 5 to 15 m, with amplitudes of about half a meter and periods of  $\sim 10$  min. The complex nature of the fluctuations in the records does not allow a reliable estimate of the wave arrival time at the system buoys. The optimal window is the ratio of the distance between the buoys (136 m) to the phase velocity of the wave (0.6 m/s), which, when taking into account the minimum recorded wave period of 5 min, provides an adequate estimate of 4 min. In the maximum gradient area, the  $9^\circ \text{C}$  isotherm was selected (Fig. 5, *a*). The moving dispersion of its occurrence depths is shown in Fig. 5, *b*.

All buoys of the drifting system show successive local maxima, which correspond to waves of a similar shape in the isotherm fluctuation records. Buoy 1 registered a wave at 12:01:00 (UTC) ( $t_1$ ), buoy 3 registered a wave at 12:11:10 ( $t_2$ ), buoy 2 registered a wave at 12:11:40 ( $t_3$ ). Such a small delay is associated with the direction of wave packet propagation, the small distance between the buoys and the relatively high phase velocity of the waves. The phase velocity calculated using expression (1) was 0.11 m/s, and the direction of propagation calculated using expression (2) was  $14^\circ$ . Taking into account the drift speed (0.53 m/s) and direction ( $65^\circ$ ), the resulting wave propagation speed was 0.6 m/s, and the direction was  $57^\circ$  (Fig. 5, *c*). The obtained phase velocity is close to the estimates obtained in the two-layer model. The propagation direction corresponds to the position and order of registration of the dispersion maxima on the buoy drift map (Fig. 5, *c*), and is also similar to the general direction of propagation of SIW packet manifestations recorded from satellite data in the area under consideration [22, 23].

## Conclusion

The paper describes a new hydrophysical measuring system based on an array of surface-drifting temperature-profiling buoys. The main advantages of this system are its mobility, ease of installation, and the ability to track the system's status in real time via a satellite communication channel. The disadvantages include the lack of a standard ability to change the position of the temperature sensors by depth. It is worth noting that the presented measuring system is suitable for recording a wide range of processes and phenomena occurring in the ocean, such as frontal and eddy dynamics.

Methodological features of estimating the speed and direction of internal waves were described. A method for determining the delay time of wave packets arriving to measuring devices was demonstrated based on the results of calculating the moving dispersion with a window determined based on the stratification conditions, the configuration of the drifting system, and the period of the recorded waves.

The results of using the system in Lake Onega and in the Kara Gate Strait are presented. Processing the measurement results using the proposed method based on calculating the moving dispersion allowed to determine the phase velocity and direction of SIW propagation.

Comparing the results obtained in Lake Onega and the Kara Gate Strait, it is worth noting that with a decrease in the distance between the buoys, the estimate of the delay in the arrival of wave packets becomes more complicated, since the difference between the moving dispersion maxima is small. This is important to take into account in subsequent work, deploying the buoys so that the distance between them is approximately equal to the length of the wave being studied.

As a result of using the Volna-DS-01 drifting system in 2022–2024, an extensive database of *in-situ* measurements was accumulated. The obtained wave characteristics in the future, together with the results of satellite observations and calculations using a high-resolution regional tidal model, will allow to determine the prevailing mechanisms of SIW generation in various areas of the Kara Sea.

The presented algorithm will be further improved. A more detailed comparative analysis of various methods for signal delay time estimation is planned, as well as the use of other methods for estimating wave speed and direction. Data on the full density profile will be used to validate phase velocity estimates, and the period of the recorded waves will be adjusted taking into account the Doppler effect.

## REFERENCES

1. Munk, W., Armi, L., Fischer, K. and Zachariasen, F., 2000. Spirals on the Sea. *Proceedings of the Royal Society A: Mathematical, Physical and Engineering Sciences*, 456(1997), pp. 1217-1280. <https://doi.org/10.1098/rspa.2000.0560>
2. Zimin, A.V., 2018. *Sub-Tidal Processes and Phenomena in the White Sea*. Moscow: GEOS Publishing, 220 p. (in Russian).

3. Ocherednik, V.V., Zatsepin, A.G., Kuklev, S.B., Baranov, V.I. and Mashura, V.V., 2020. Examples of Approaches to Studying the Temperature Variability of Black Sea Shelf Waters with a Cluster of Temperature Sensor Chains. *Oceanology*, 60(2), pp. 149-160. <https://doi.org/10.1134/S000143702001018X>
4. Serebryany, A., Khimchenko, E., Popov, O., Denisov, D., and Kenigsberger, G., 2020. Internal Waves Study on a Narrow Steep Shelf of the Black Sea Using the Spatial Antenna of Line Temperature Sensors. *Journal of Marine Science and Engineering*, 8(11), 833. <https://doi.org/10.3390/jmse8110833>
5. Kozlov, I.E., Kopyshov, I.O., Frey, D.I., Morozov, E.G., Medvedev, I.P., Shiryborova, A.I., Silvestrova, K.P., Gavrikov, A.V., Ezhova, E.A. [et al.], 2023. Multi-Sensor Observations Reveal Large-Amplitude Nonlinear Internal Waves in the Kara Gates, Arctic Ocean. *Remote Sensing*, 15(24), 5769. <https://doi.org/10.3390/rs15245769>
6. Stepanyuk, I.A., 2002. *Methods for Measuring the Parameters of Internal Sea Waves*. Saint Petersburg: RGGMU Publishing, 138 p. (in Russian).
7. Motyzhev, S.V., Lunev, E.G. and Tolstosheev, A.P., 2017. The Experience of Using Autonomous Drifters for Studying the Ice Fields and the Ocean Upper Layer in the Arctic. *Physical Oceanography*, (2), pp. 51-64. <https://doi.org/10.22449/1573-160X-2017-2-51-64>
8. Tolstosheev, A.P., Lunev, E.G. and Motyzhev, V.S., 2008. Development of Means and Methods of Drifter Technology Applied to the Problem of the Black Sea Research. *Oceanology*, 48(1), pp. 138-146. <https://doi.org/10.1007/s11491-008-1016-4>
9. Zimin, A.V., Rodionov, A.A., Motyzhev, S.V., Lunev, E.G. and Tolstosheev, A.P., 2021. A System to Monitor Characteristics of Hydrophysical Fields in the Sub-Mesoscale Variability Interval. In: MHI, 2021. *Proceedings of All-Russian Scientific Conference. The Seas of Russia: Year of Science and Technology in the RF – United Nations Decade of Ocean Science for Sustainable Development*. Sevastopol, pp. 246-247 (in Russian).
10. Svergun, E.I., Zimin, A.V., Lunyov, E.G., Tolstosheev, A.P. and Bezgin, A.A., 2023. A Method for Estimating the Characteristics of Short-Period Internal Waves Based on the Data of a Drifting buoy Array. In: MHI, 2023. *Proceedings of All-Russian Scientific Conference. The Seas of Russia: From Theory to Practice of Oceanological Research*. Sevastopol, pp. 102-103 (in Russian).
11. Centurioni, L.R., 2010. Observations of Large-Amplitude Nonlinear Internal Waves from a Drifting Array: Instruments and Methods. *Journal of Atmospheric and Oceanic Technology*, 27(10), pp. 1711-1731. <https://doi.org/10.1175/2010JTECHO774.1>
12. Lee, O.S., 1961. Observations on Internal Waves in Shallow Water. *Limnology and Oceanography*, 6(3), pp. 312-321. <https://doi.org/10.4319/lo.1961.6.3.0312>
13. Johannessen, O.M., Sandven, S., Chunchuzov, I.P. and Shuchman, R.A., 2019. Observations of Internal Waves Generated by an Anticyclonic Eddy: A Case Study in the Ice Edge Region of the Greenland Sea. *Tellus A: Dynamic Meteorology and Oceanography*, 71(1), 1652881. <https://doi.org/10.1080/16000870.2019.1652881>
14. Gong, Q., Chen, L., Diao, Y., Xiong, X., Sun, J. and Lv, X., 2023. On the Identification of Internal Solitary Waves from Moored Observations in the Northern South China Sea. *Scientific Reports*, 13(1), 3133. <https://doi.org/10.1038/s41598-023-28565-5>
15. Sevostyanov, P.A., Samoilova, T.A. and Rodin, A.A., 2019. [Sequential Regressions in the Analysis and Forecasting of Time Series Variability]. In: Vitebsk State Technological University, 2019. *Innovative Technologies in Textile, Shoe, Knitwear and Clothing Industry. Proceedings of Scientific-and-Technical Conference*. Vitebsk, pp. 305-307 (in Russian).
16. Sverdlík, L.G., 2021. Identification of Pre-Seismic Atmospheric Perturbations Using Modified STA/LTA Criterion. *Current Problems of Remote Sensing of the Earth from Space*, 18(3), pp. 141-149. <https://doi.org/10.21046/2070-7401-2021-18-3-141-149> (in Russian).

17. Saidov, O.A., 2014. Monitoring of Geochemical Parameters Variations in the Region of Dagestan Wedge in Connection with Seismic Events. *Monitoring. Science and Technology*, 4(21), pp. 71-75 (in Russian).
18. Khodyaev, A.V., Shevyrnogov, A.P., Vysotskaya, G.S. and Kozikova, O.S., 2011. Using Moving Variance Method to Detect Ocean Currents from Space. *Journal of Siberian Federal University. Engineering and Technologies*, 4(2), pp. 179-184.
19. Konyaev, K.V. and Sabinin, K.D., 1992. *Waves inside the Ocean*. Saint Petersburg: Gidrometeoizdat, 269 p. (in Russian).
20. Zhegulin, G.V., Zimin, A.V. and Rodionov, A.A., 2016. Analysis of the Dispersion Dependence and Vertical Structure of Internal Waves in the White Sea in Experimental Data. *Fundamental and Applied Hydrophysics*, 9(4), pp. 47-59 (in Russian).
21. Meng, J., Zhang, H., Sun, L. and Wang, J., 2024. Remote Sensing Techniques for Detecting Internal Solitary Waves: A Comprehensive Review and Prospects. *IEEE Geoscience and Remote Sensing Magazine*, 12(4), pp. 46-78. <https://doi.org/10.1109/MGRS.2024.3402673>
22. Kozlov, I.E., Kudryavtsev, V.N., Zubkova, E.V., Atadjanova, O.A., Zimin, A.V., Romanenkov, D.A., Shapron, B. and Myasoedov, A.G., 2014. Generation Sites of Nonlinear Internal Waves in the Barents, Kara and White Seas from Spaceborne SAR Observations. *Current Problems of Remote Sensing of the Earth from Space*, 11(4), pp. 338-345 (in Russian).
23. Kopyshov, I.O., Kozlov, I.E., Shiryborova, A.I. and Myslenkov, S.A., 2023. Properties of Short-Period Internal Waves in the Kara Gates Strait Revealed from Spaceborne SAR Data. *Russian Journal of Earth Sciences*, 23, ES0210. <https://doi.org/10.2205/2023ES02S110>

*About the authors:*

**Egor I. Svergun**, Researcher, Shirshov Institute of Oceanology, Russian Academy of Sciences, (30, 1st Line of Vasilievsky Island, Saint Petersburg, 119053, Russian Federation), CSc. (Geogr.), **WoS ResearcherID: AAC-7289-2020**, **Scopus Author ID: 57195066881**, **ORCID ID: 0000-0002-9228-5765**, **SPIN-code: 3212-7041**, [egor-svergun@yandex.ru](mailto:egor-svergun@yandex.ru)

**Alexey V. Zimin**, Senior Researcher, Shirshov Institute of Oceanology, Russian Academy of Sciences (30, 1st Line of Vasilievsky Island, Saint Petersburg, 119053, Russian Federation), DSc. (Geogr.), Professor, Saint Petersburg State University (7/9 Universitetskaya Embankment, Saint Petersburg, 199034, Russian Federation), **ORCID ID: 0000-0003-1662-6385**, **WoS ResearcherID: C-5885-2014**, **Scopus Author ID: 55032301400**, **SPIN-code: 9833-3460**, [zimin2@mail.ru](mailto:zimin2@mail.ru)

**Sergey V. Motyzhev**, Chief Researcher, Sevastopol State University (33 Universitetskaya Str., Sevastopol, 299053, Russian Federation), DSc. (Tech.), **ORCID ID: 0000-0002-8438-2602**, **Scopus Author ID: 6507354504**, **SPIN-code: 1999-2976**, [motyzhev@marlin-yug.com](mailto:motyzhev@marlin-yug.com)

**Aleksey P. Tolstosheev**, Leading Researcher, Sevastopol State University (33 Universitetskaya Str., Sevastopol, 299053, Russian Federation), DSc. (Tech.), **ORCID ID: 0000-0002-0771-0879**, **ResearcherID: G-1901-2014**, **Scopus Author ID: 23994548500**, **SPIN-code: 8885-3906**, [tolstosheev@marlin-yug.com](mailto:tolstosheev@marlin-yug.com)

**Evgeniy G. Lunev**, Leading Researcher, Sevastopol State University (33 Universitetskaya Str., Sevastopol, 299053, Russian Federation), DSc. (Tech.), **ORCID ID: 0000-0002-7138-3024**, **Scopus Author ID: 23994266100**, **SPIN-code: 9627-6497**, [lunev@marlin-yug.com](mailto:lunev@marlin-yug.com)

**Mihail S. Volikov**, Researcher, Sevastopol State University (33 Universitetskaya Str., Sevastopol, 299053, Russian Federation), **ORCID ID: 0000-0003-4307-0423**, **ResearcherID: ABI-9792-2022**, **SPIN-code: 7799-5042**, [volikov@marlin-yug.com](mailto:volikov@marlin-yug.com)

Submitted 19.09.2024; approved after review 11.10.2024;  
accepted for publication 13.03.2025.

*Contribution of the co-authors:*

**Egor I. Svergun** – carrying out experimental studies, data collection and systematization, analysis of measurement data, selection and analysis of literature, preparation of the article text, creation of figures

**Alexey V. Zimin** – carrying out experimental studies, selection and analysis of literature, scientific supervision, critical analysis and revision of the text

**Sergey V. Motyzhev** – general scientific supervision, development and scientific substantiation of the research concept, analysis of materials, discussion of results

**Aleksey P. Tolstosheev** – carrying out laboratory studies, development and implementation of information and measuring system, metrological support, analysis of materials, discussion of the results, updating of the paper text

**Evgeniy G. Lunev** – development and implementation of information and measuring system, analysis of materials, discussion of the results, updating of the paper text

**Mihail S. Volikov** – carrying out experimental studies, development and implementation of information and measuring system, development of software, discussion of the results

*The authors have read and approved the final manuscript.*

*The authors declare that they have no conflict of interest.*